

# Accepted Manuscript

Synthesis and molecular docking of new roflumilast analogues as preferential-selective potent PDE-4B inhibitors with improved pharmacokinetic profile

Bahia A. Moussa, Asmaa A. El-Zaher, Mohamed K. El-Ashrey, Marwa A. Fouad



PII: S0223-5234(18)30168-5

DOI: [10.1016/j.ejmech.2018.02.038](https://doi.org/10.1016/j.ejmech.2018.02.038)

Reference: EJMECH 10215

To appear in: *European Journal of Medicinal Chemistry*

Received Date: 14 December 2017

Revised Date: 8 February 2018

Accepted Date: 12 February 2018

Please cite this article as: B.A. Moussa, A.A. El-Zaher, M.K. El-Ashrey, M.A. Fouad, Synthesis and molecular docking of new roflumilast analogues as preferential-selective potent PDE-4B inhibitors with improved pharmacokinetic profile, *European Journal of Medicinal Chemistry* (2018), doi: 10.1016/j.ejmech.2018.02.038.

This is a PDF file of an unedited manuscript that has been accepted for publication. As a service to our customers we are providing this early version of the manuscript. The manuscript will undergo copyediting, typesetting, and review of the resulting proof before it is published in its final form. Please note that during the production process errors may be discovered which could affect the content, and all legal disclaimers that apply to the journal pertain.



# **Synthesis and Molecular Docking of New Roflumilast Analogues as Preferential-Selective Potent PDE-4B Inhibitors with Improved Pharmacokinetic Profile**

*Bahia A. Moussa, Asmaa A. El-Zaher, Mohamed K. El-Ashrey and Marwa A. Fouad\**

Pharmaceutical Chemistry Department, Faculty of Pharmacy, Cairo University, Kasr El-Eini  
Street, P.O. Box 11562, Cairo, Egypt

---

*\*Corresponding author: ORCID Marwa Fouad: 0000-0003-3227-8683*

*E-mail address: marwa.fouad@pharma.cu.edu.eg*

*Tel: +201222441198*

**Abstract**

In the present work, we designed and synthesized new roflumilast analogues with selective PDE-4B inhibition activity and improved pharmacokinetic properties. The unsubstituted benzo[d]thiazol-2-yl and -6-yl benzamide derivatives (**4a** and **6a**) showed both good potency and preferential selectivity for PDE-4B. More remarkably, **6c** revealed 6 times preferential PDE-4B/4D selectivity with a significant increase of *in vitro* cAMP and good % inhibition of TNF- $\alpha$  concentration. In addition, the *in vitro* pharmacokinetics of **6c** showed good metabolic stability with *in vitro* CL<sub>int</sub> (5.67 mL/min/kg) and moderate % plasma protein binding (53.71%). This was reflected onto increased *in vivo* exposure with a half-life greater than roflumilast by 3 folds (21 h) and a C<sub>max</sub> value of 113.958  $\mu$ g/mL. Molecular docking attributed its good activity to its key binding interactions in PDE-4B active site with additional hydrogen bonding with amino acids lining the metal pocket. Summing up, **6c** can be considered as suitable candidate for further investigation for the treatment of COPD.

**Keywords:** Phosphodiesterase 4B inhibitor; 2-aminobenzothiazole; 6-aminobenzothiazole; 2-aminothiazole; Chronic Obstructive Pulmonary disorder; Pharmacokinetics

## 1 Introduction

Chronic obstructive pulmonary disease (COPD) has an increasing rate of morbidity and mortality that it kills about 3 million people all over the world every year [1,2]. Many inflammatory cells and mediators participate in COPD symptoms such as bronchitis and emphysema, so prevention of their activation or antagonizing their receptors become a challenge for a medicinal chemist to find new chemical entities (NCEs) that play this role [3–5].

Many treatments had been developed for COPD as inhaled corticosteroids [6–9], inhibitors of inducible nitric oxide synthase (i-NOS) [10], leukotriene inhibitors [11,12], adhesion-molecule blockers [13], chemokine inhibitors [14], TNF $\alpha$  inhibitors [15], NF $\kappa$ B inhibitors [16], p38 MAPK inhibitors [17], Phosphoinositide 3-kinase (PI3K) inhibitors [18] and Peroxisome proliferator-activated receptors (PPARs) activators [19–21].

The discovery of selective phosphodiesterase 4 (PDE-4) inhibitors as a way for treatment of inflammation in COPD patients was prompted when it has been observed that raising the intracellular levels of 3'5'-cyclic adenosine monophosphate (cAMP) can inhibit the functions of inflammatory cells and also due to the wide distribution of PDE-4 enzymes in inflammatory cells and in the lung [22–24],

There are 11 distinct enzymes of PDEs [25,26] in which PDE-4 specifically inactivates cAMP which is highly expressed in inflammatory cells, and so, inhibitors of PDE-4 enzyme cause a decrease in inflammatory response which is increased in COPD [27,28], PDE-4 enzymes are classified into 4 subtypes (4A-D) which show a similarity of 78% in the active catalytic site [29].

It has been revealed that selective inhibition of PDE-4B showed a potent anti-inflammatory effect not associated with emesis side effect accompanied with the inhibition of PDE-4D enzyme [30–32].

Roflumilast was marketed in the USA in 2012 for the treatment of COPD as a PDE-4 inhibitor [33,34]. Though, its side effects, such as gastrointestinal upsets, headache, and weight loss limited its therapeutic potential [35].

Roflumilast is rapidly metabolized to its active metabolite, roflumilast N-oxide, which has twofold to threefold specificity and potency less than roflumilast [36]. The main cytochrome P450 enzymes that are responsible for the conversion of roflumilast to its N-oxide metabolite are CYP3A4 and 1A2 [37,38]. As the activity of these two enzymes can be affected by interindividual variables, so it is can be predicted that these variables can affect roflumilast pharmacokinetics [39–41].

As reported [42,43], “PDE-4B and PDE-4D enzymes are composed of a compact  $\alpha$ -helical structure that forms three subdomains. The PDE active site forms a deep pocket at the junction of these three subdomains. The active site can be subdivided into three pockets: a metal binding pocket which contains magnesium and zinc ions in addition to highly conserved hydrophobic and polar residues that coordinates the metal ions (M pocket), a solvent filled side pocket which consists mainly of hydrophilic amino acids and is filled with a network of water molecules in most of the inhibitor complexes (S pocket), and a third pocket containing the invariant purine-selective glutamine and a pair of conserved residues that form a hydrophobic clamp (Q pocket)”.

In an effort to discover PDE4B/4D selective inhibitors, a 2-arylpyrimidine derivative **I** was identified as a selective and potent PDE4B inhibitor with an  $IC_{50}$  of sub-micromolar range (0.19  $\mu$ M) and a potential 10-fold selectivity over PDE4D.[44] By high throughput screening, tetrahydrobenzothiophene bisamide **II** was found to be a potent and modest PDE4B/4D-selective inhibitor (PDE4B/4D  $pIC_{50}$  6.7/6.5).[45] The pyridazino[4,5-b]indolizine analogue **III** was found to possess a 23-fold selectivity for PDE4B over PDE4D.[46] Compound **IV** was identified

as an orally active PDE4B selective inhibitor over PDE4D both in humans (80-fold selective) and mice (29-fold selective) (Figure 1).[47]

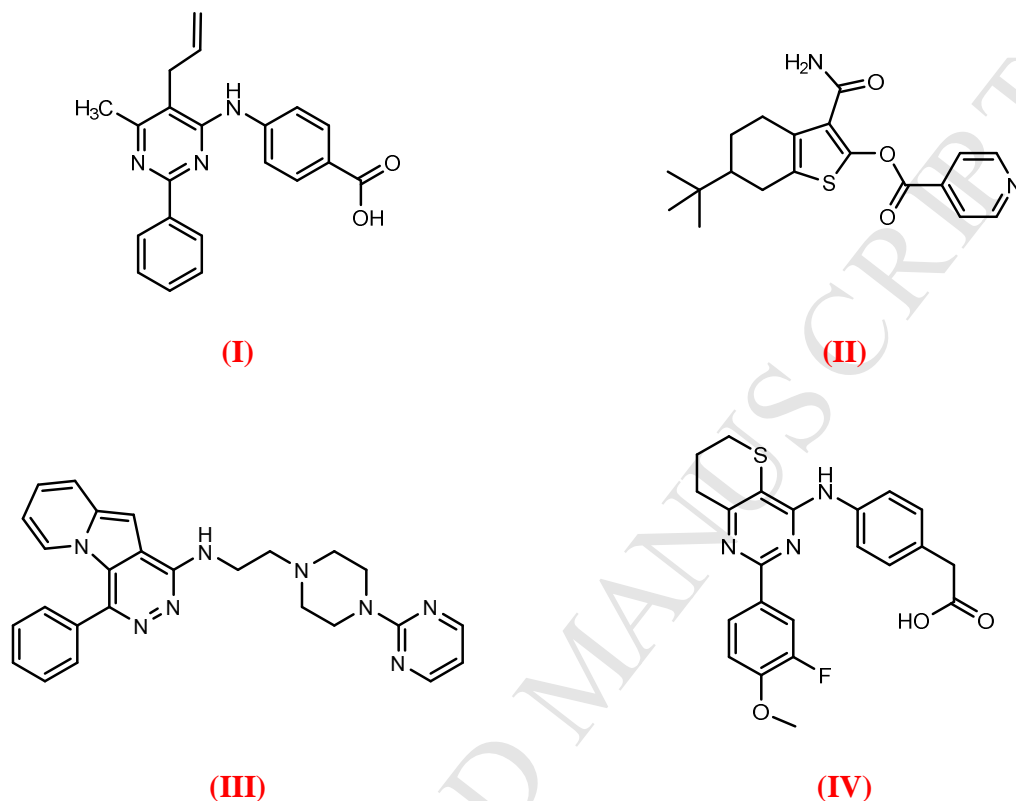


**Figure 1.** Structures of some reported PDE4B/4D selective inhibitors

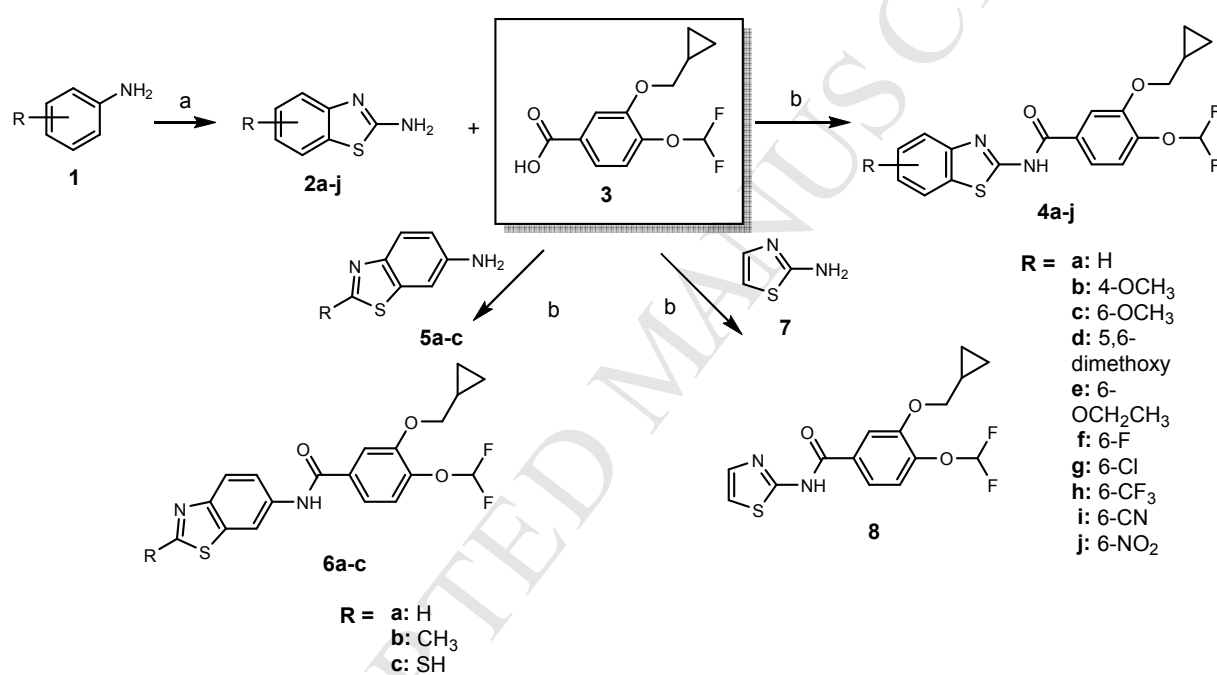
Reported research for the discovery of new PDE-4 inhibitors showed that some heterocyclic groups, such as morpholine, phthalazinone, and benzothiazole could play the role of pyridine moiety in roflumilast in affecting biological activity [48–52].

Accordingly, we can design a NCE through the hybridization of two reported pharmacophores into one molecule [53–55]. Therefore, these previously mentioned facts urge the need for the discovery of novel selective PDE-4B inhibitors with good potency and better metabolic profile. This work deals with synthesis of novel series **4**, **6** and **8** through hybridization of the pharmacophores, 3-(cyclopropylmethoxy)-4-(difluoromethoxy)benzoic acid with amino-2-thiazole, 2- or 6-benzothiazole via amide linkage (Chart. 1), hoping to obtain new PDE-4B



yield was obtained by using the one pot amide synthesis reaction by treating the starting acid **3** with thionyl chloride and the excess was then removed easily by distillation. Target compounds were then obtained through coupling reaction [64] with the formed acid chloride by the addition of the corresponding amine derivatives **2a-j**, **5a-c** and **7** in dry benzene in the presence of anhydrous potassium carbonate.

### Scheme 1. Preparation of Target Compounds



**a:** NH<sub>4</sub>SCN / HCl / Br<sub>2</sub> / glacial acetic acid, **b:** SOCl<sub>2</sub> / Anhyd K<sub>2</sub>CO<sub>3</sub>, Dry Benzene

## 2.2 Biological evaluation

All the newly synthesized compounds were evaluated for their ability to inhibit the PDE-4B enzyme using Roflumilast as positive control. The IC<sub>50</sub> values were determined by nonlinear regression analysis of their inhibition curves and shown in table 1. All the synthesized compounds showed potent PDE-4B inhibition activity in the nanomolar range. The three

compounds, **4a**, **6a** and **6c** showed higher potency than Roflumilast with subnanomolar IC<sub>50</sub> values.

Thorough study of the structure-activity relationship of the unsubstituted derivatives (**4a**, **6a** and **8**) revealed that **4a** and **6a** showed good potency with no significant inhibition difference from Roflumilast while replacement of the benzothiazole ring in either **4a** or **6a** with the simplified thiazole ring (**8**) significantly decreased the potency of inhibition. Moreover, substitution of the benzothiazole ring in series **4** with either an electron donating group such as alkoxy or dialkoxy group or an electron withdrawing group such as halogens, trifluoromethyl, cyano or nitro group (**4b-j**) significantly decreased the potency of the unsubstituted compound (**4a**). The trifluoromethyl and the nitro substituted 2-aminobenzothiazole derivatives (**4h** and **4j**, respectively) exhibited the lowest potency in this series ( $p < 0.05$ ).

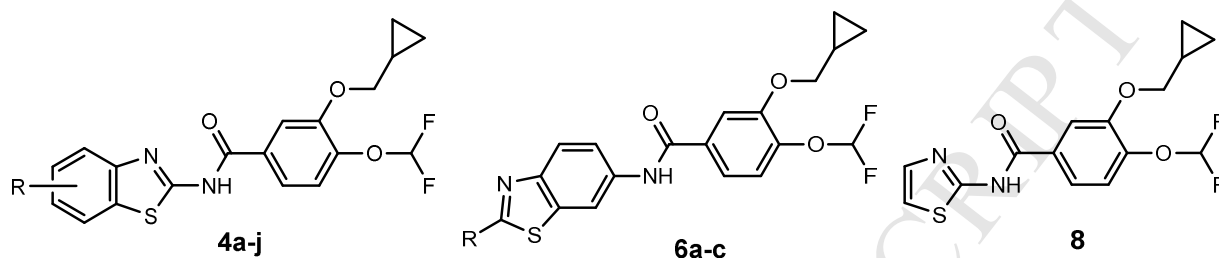
On the other hand, substitution of 6-aminobenzothiazole derivatives (**6a-c**) at position 2 with a methyl group (**6b**) significantly increased the IC<sub>50</sub> value of the unsubstituted derivative while substitution with a mercapto group (**6c**) showed good potency with no significant difference with the parent compound (**6a**) ( $p < 0.05$ ).

Compounds (**4a**, **6a** and **6c**) were selected to study their PDE-4B/4D selectivity (Table 2, Figure 2). All the 3 compounds showed preferential selectivity towards PDE-4B isozyme compared to the reference compound.

As **4a** and **6c** showed the highest selectivity, they were subjected to further investigations and their effect on TNF- $\alpha$  and cAMP levels were studied and compared to those of Roflumilast. Both, **4a** and **6c**, exhibited an increase in the level of cAMP higher than that of roflumilast. **6c** significantly increases cAMP level for more than 2 folds than roflumilast with a significant difference at  $p < 0.05$ . Decreasing TNF- $\alpha$  level assists in anti-inflammatory action of PDE-4

inhibitors. The synthesized derivative **6c** showed a higher level of inhibition of TNF- $\alpha$  than **4a** derivative (Table 2, Figure 2).

**Table 1. PDE-4B inhibitory data**



Compd	R	IC <sub>50</sub> [nM]
<b>Roflumilast</b>	-	0.90
<b>4a</b>	H	0.57
<b>4b</b>	4-OCH <sub>3</sub>	1.06
<b>4c</b>	6-OCH <sub>3</sub>	2.28*
<b>4d</b>	5,6-Dimethoxy	1.17
<b>4e</b>	6-OCH <sub>2</sub> CH <sub>3</sub>	2.92*
<b>4f</b>	6-F	1.87*
<b>4g</b>	6-Cl	1.22
<b>4h</b>	6-CF <sub>3</sub>	5.23*
<b>4i</b>	6-CN	1.28
<b>4j</b>	6-NO <sub>2</sub>	8.67*
<b>6a</b>	H	0.68
<b>6b</b>	2-CH <sub>3</sub>	1.26
<b>6c</b>	2-SH	0.75
<b>8</b>	-	1.60*

\* IC<sub>50</sub> is significantly different from that of Roflumilast at P<0.05

**Table 2. Biological evaluation results, S9 Stability and human plasma protein binding of compounds: Roflumilast, 4a, 6a and 6c**

	<b>Rof</b>	<b>4a</b>	<b>6a</b>	<b>6c</b>
<b>PDE-4B IC<sub>50</sub></b> <b>(nM)</b>	0.90	0.57	0.68	0.75
<b>PDE-4D IC<sub>50</sub></b> <b>(nM)</b>	0.56	5.07	2.73	4.54
<b>4D/4B Ratio</b>	0.66	8.89	4.01	6.05
<b>TNF-<math>\alpha</math></b> <b>(%Inhibition)</b>	70.32	58.61	ND	67.79
<b>cAMP</b> <b>(pM/mL)</b>	1.898	2.676	ND	4.446
<b><i>In vitro</i> t<sub>1/2</sub></b> <b>(min.)</b>	12.29	42.27	63.01	247.55
<b>CL<sub>int</sub></b> <b>(mL/min/kg)</b>	114.19	33.20	22.27	5.67
<b>%Bound</b>	98.49	100	96.39	53.71

\*ND: not done

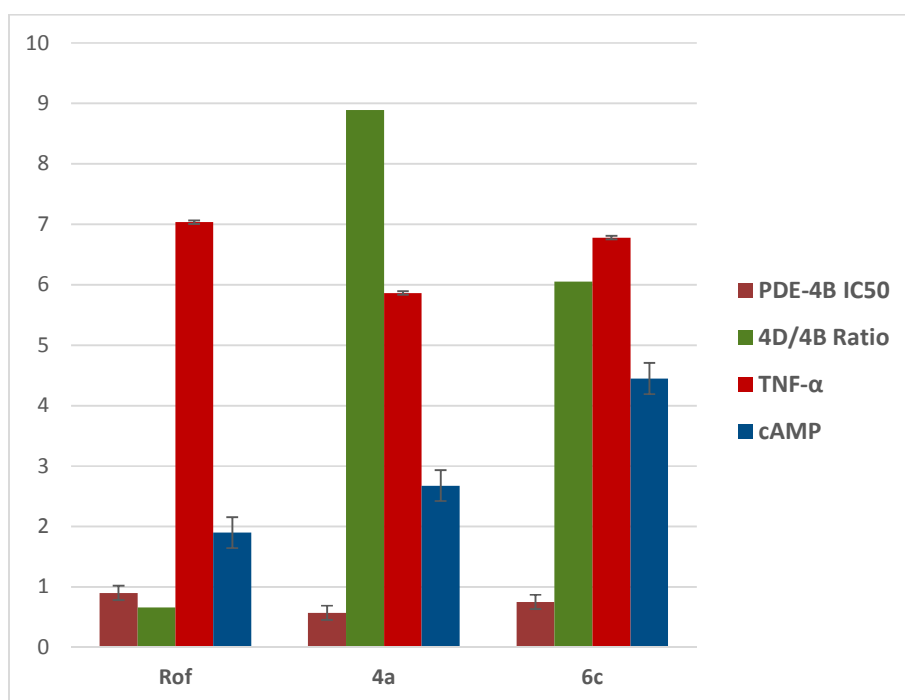


**Figure 2.** *In vitro* biological results of **4a** and **6c** compared to Roflumilast.

### 2.3 Molecular docking study

Many crystal structures for PDE-4B and PDE-4D isozymes co-crystallized with different inhibitors are available in the protein data bank. To undergo the docking study, we retrieved the X-ray crystal structure of PDE-4B (PDB ID: 1XMU, resolution 2.3 Å) and PDE-4D (1XOQ, resolution 1.83 Å) [42] that are in complex with roflumilast.

Validation of the molecular docking setup was carried out by re-docking of roflumilast into the PDE-4B and PDE-4D active sites. Nearly the same binding of the co-crystallized ligand was reproduced in the validation step including key interactions [42] thus indicating that the used setup is suitable for our docking study. As the co-crystallized ligand, the dialkoxyphenyl ring of the docked roflumilast is inserted in between the hydrophobic clamp: Phe446 and Ile410 in PDE-4B (Phe372 and Ile336 in PDE-4D) Q pocket. Also, the dichloropyridyl group forms one H bond to a water molecule coordinated to  $Mg^{2+}$  in the M pocket (Supporting information, Figure S1).

This was also confirmed by the small RMSD of 0.4555Å between the co-crystallized ligand and the reproduced docked pose (energy score (S) = -25.1316 kcal/mol) for PDE4B (PDB ID: 1XMU) and RMSD of 0.7788Å (energy score (S) = -24.7497 kcal/mol) for PDE4D (PDB ID: 1XOQ).

By comparing docking of the new compounds with the reference compound in PDE-4B active site, all the synthesized compounds interact through the oxygens of the dialkoxyphenyl moieties with the NH of the  $\gamma$ -carboxamide group of Gln443 which is involved in nucleotide recognition, through a single or bidentate H bonds accommodating the dialkoxyphenyl ring in the hydrophobic clamp. The difluoromethoxy group is inserted into the small Q1 pocket and the cyclopropylmethoxy group occupies the larger hydrophobic Q<sub>2</sub> pocket and forms a hydrophobic interaction with Phe446. Moreover, the primary aromatic ring exhibited CH- $\pi$  interaction with Ile410. These interactions play an important role in the stabilization of the inhibitor at the active site (Supporting information, Figure S2-S8).

All the compounds are generally oriented such that their benzothiazole or thiazole moiety is directed into the metal binding pocket. In contrast to compound **8**, both 2-amino and 6-aminobenzothiazole derivatives (series **4** and **6**) perform H bond interaction with a water molecule coordinated with Mg<sup>2+</sup> cation through the  $\pi$  electrons of the benzothiazole moiety. This orientation may interfere with the approach of cAMP to the catalytic domain.

Moreover, Compound **6c** exhibited additional two H bonds with the  $\alpha$ -carboxamido group of Asn283 and the  $\gamma$ -carboxylate group of Glu304 through the 2-SH group as hydrogen acceptor and hydrogen donor, respectively. These two residues are among those lining the metal binding pocket (Figure 3).

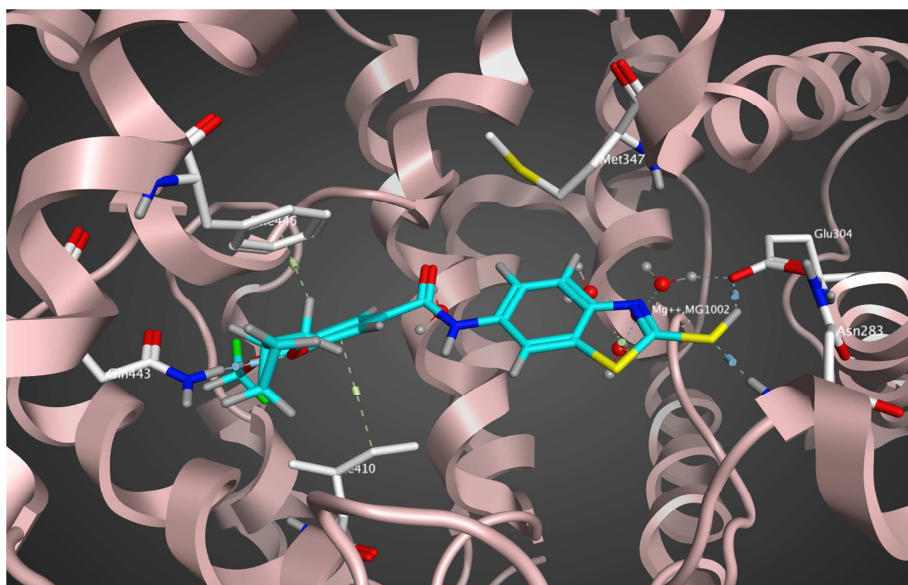


**Figure 3.** 3D Representation of the interaction of the docked **6c** in the active site of PDE-4B enzyme (PDB ID: 1XMU) using Molecular Operating Environment (MOE, 10.2008) software

In summary, this set of interactions ensures that the newly synthesized derivatives achieve a strong binding to the PDE-4B enzyme comparable to that of the reference compound and thus, good biological activity. The difference in experimental  $IC_{50}$  values among tested compounds is well reflected in their docking scores (Table 3).

**Table 3. Docking energy scores (S) in kcal/mol for the newly synthesized compounds and the reference compound in PDE-4B and PDE-4D enzymes.**

Compd	Energy score (S)	Energy score (S)
	kcal/mol (PDE4B)	kcal/mol (PDE4D)
Roflumilast	-25.13	-24.75
<b>4a</b>	-26.35	-24.58
<b>4b</b>	-22.18	-26.15
<b>4c</b>	-20.53	-24.64
<b>4d</b>	-22.93	-22.63
<b>4e</b>	-20.89	-23.06
<b>4f</b>	-23.90	-24.11
<b>4g</b>	-22.66	-20.08
<b>4h</b>	-19.95	-20.09
<b>4i</b>	-22.08	-20.32
<b>4j</b>	-19.05	-22.20
<b>6a</b>	-25.89	-24.87
<b>6b</b>	-22.38	-25.95
<b>6c</b>	-25.59	-23.68
<b>8</b>	-19.70	-21.96

Recent studies have indicated overall similarity of the catalytic domain in the PDE4 subfamilies with a high degree of sequence conservation [42,65]. Although the binding pattern of the new compounds in PDE-4B and PDE-4D is comparable except for **6c** (Supporting information, Figure S9-S12), the difference between the docking scores of roflumilast, **4a**, **6a**

and **6c** when docked in PDE-4B and PDE-4D reflects, to a great extent, the *in vitro* experimental IC<sub>50</sub> values difference thus ascertaining their preferential binding affinity.

#### 2.4 *In vivo* pharmacokinetic study

Pharmacokinetic parameters were estimated for the most potent synthesized derivatives **4a**, **6a** and **6c** in male Sprague-Dawley rats using Roflumilast as the reference compound. The three compounds showed good pharmacokinetic parameters with a C<sub>max</sub> value of 95.491, 86.241 and 113.958 µg/mL comparable to that of roflumilast and an AUC value of 594.078, 892.133 and 622.382 µg.h/mL, respectively, higher than that of roflumilast after a subcutaneous dose of 1 mg/kg. In addition, they demonstrated relatively lower clearance rate (CL= 1.250, 0.619 and 0.960 mL/h.kg) than that of the reference drug. These data suggested that replacement of the dichloropyridyl moiety of roflumilast, which is subjected to rapid N-oxidation, by a benzothiazole ring might attribute to the improvement of the pharmacokinetic profile. Moreover, **6c** demonstrated an excellent pharmacokinetic profile with the highest half-life > 21 h and the highest maximum plasma concentration, Table 4, Figure 4.

**Table 4. Sprague-Dawley rat PK Profile of Roflumilast and compounds 4a, 6a and 6c**

Parameter	Rof	4a	6a	6c
Rat no.	6	6	6	6
Dose level (mg/kg)	1	1	1	1
<i>t</i> <sub>1/2</sub> (h)	6.938	9.819	21.959	21.991
T <sub>max</sub> (h)	1	1	2	2
C <sub>max</sub> (µg/mL)	108.751	95.491	86.241	113.958
AUC <sub>0-t</sub> (µg.h/mL)	449.426	594.078	892.133	622.382
AUC <sub>0-∞</sub> (µg.h/mL)	499.506	799.823	1616.333	1041.629
V <sub>d</sub> (mL/kg)	20.039	17.712	19.600*	30.459

CL (mL/h.kg)	2.002	1.250	0.619	0.960
--------------	-------	-------	-------	-------

\* Not significantly different from that of Roflumilast at  $P < 0.05$

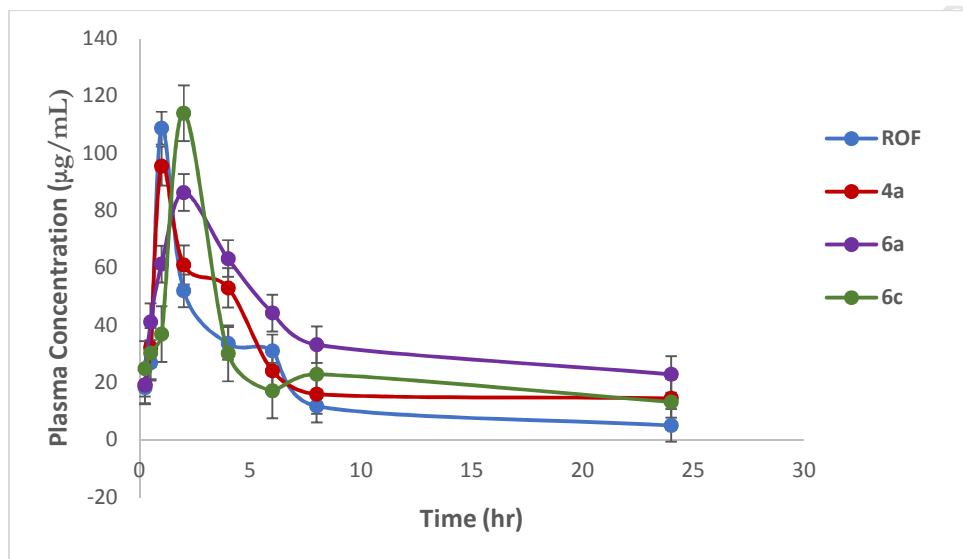


**Figure 4.** Time-dependent plasma concentrations of **ROF**, **4a**, **6a** and **6c** after subcutaneous administration to male Sprague-Dawley rats.

## 2.5 *In vitro* pharmacokinetic studies

### 2.5.1 Metabolic stability

The most promising inhibitors of PDE4B enzyme, **4a**, **6a**, **6c**, were tested for their metabolic stability in rat subcellular fraction and compared to roflumilast. This was carried out by incubation of each inhibitor with the S9 fraction in the presence of the co-factor NADPH for different time intervals to test their phase I metabolic stability. The *in vitro* half-life ( $t_{1/2}$ ) and the intrinsic clearance ( $CL_{int}$ ) were calculated (Table 2). By comparing the 3 tested compounds to roflumilast ( $t_{1/2} = 12.29$  min), it appears that they all have a better metabolic stability especially the 2-mercapto-6-aminobenzothiazole derivative (**6c**) ( $t_{1/2} = 247.55$  min) which showed a half-life time that is 20-fold greater than that of Roflumilast and an encouraging *in vitro* clearance of 5.67 mL/min/kg. Removal of the mercapto group decreased the half-life of the unsubstituted 6-

aminobenzothiazole derivative (**6a**) ( $t_{1/2}$ = 63.01 min) 4-folds. Moreover, the unsubstituted 2-aminobenzothiazole derivative (**4a**) showed a moderate metabolic stability ( $t_{1/2}$ = 42.27 min).

Thus, further investigation was needed in order to predict the possible metabolites of compounds **4a** and **6a** and also to evaluate their metabolic fate. Incubation samples (60 min) were treated and then injected onto UPLC-MS/MS. Metabolites were predicted according to the reported roflumilast metabolism and expected benzothiazole biotransformations [66,67]. In case of **4a**, the detected metabolic product was derived from aromatic hydroxylation of the benzothiazole moiety (405.07  $m/z$ ). For **6a**, aromatic hydroxylated metabolite (405.11  $m/z$ ) in addition to the cleaved benzothiazole (381.09  $m/z$ ) were detected (Supporting Information, Figure S13-S15).

As **6c** was the most metabolically stable analog with 84.2% intact after 60 min compared to **4a** and **6a** (36.4% and 36.8%, respectively), it can be deduced that substitution at position 2 with the mercapto group may play an important role in protecting the compound against phase I metabolism.

### 2.5.2 Human plasma protein binding

Drug protein binding can impact both the pharmacokinetics and pharmacodynamics of a drug. Thus, estimation of plasma protein binding is an important part of characterization of a new chemical entity during its development into a drug [68]. Equilibrium dialysis is considered to be the best method for the estimation of drug protein binding. Thus, compounds **4a**, **6a** and **6c** were selected to investigate their plasma protein binding *in vitro* using equilibrium dialysis method and the %Bound for each compound was compared to that of reference compound Roflumilast (Table 2). Compounds **4a** and **6a** showed very high plasma protein binding (more than 95%) comparable to that of roflumilast while **6c** showed a moderate percentage of plasma protein

binding (53.71%) illustrating its availability for tissue distribution and avoiding drug-drug protein displacement interaction.

### 3 Conclusion

New benzothiazole derivatives as PDE-4B inhibitors were developed by replacing the dichloropyrid-4-yl amino moiety of roflumilast with either benzothiazol-2-yl, benzothiazol-6-yl or thiazol-2-yl amino moiety. Most of the compounds showed potent PDE-4B inhibitory activities. Moreover, **4a**, **6a** and **6c** were found to be more potent than roflumilast and subsequently selected for further investigation. One of the potent compounds, **6c**, was found to have preferential PDE-4B selectivity 6 times over PDE-4D with a significant increase of *in vitro* cAMP concentration and good % inhibition of TNF- $\alpha$  concentration. The introduction of mercapto group at 2-position (**6c**) seems to stabilize the molecule against phase I metabolism while retaining good PDE-4B IC<sub>50</sub> value and potent PDE4B/4D selectivity. the increased metabolic stability of **6c** (*in vitro*  $t_{1/2}$  = 247.55 min., Cl<sub>int</sub> = 5.67 mL/min/kg) as compared to roflumilast in rat subcellular fraction was reflected onto increased *in vivo* exposure with a half-life greater than that of roflumilast by 3 folds (21 h). In addition, it showed a moderate % of plasma protein binding (53.71%) less than that of roflumilast (98.5%). This new compound can be considered as a good drug candidate for treating COPD.

## 4 Experimental

### 4.1 Chemistry

Solvents and chemicals were purchased from commercial sources and used without purification. Melting points were recorded using Stuart SMP3 Digital Melting Point apparatus. All the reactions were followed up by TLC using silica gel F254 plates (Merck), using chloroform: methanol 9.5:0.5 or pure chloroform as eluting system and were visualized by UV-

lamp. All final compounds had a percentage purity of at least 95%, and this was verified using UPLC-MS/MS conducted on a Waters TQD LC-MS-MS system with a mobile phase consisting of acetonitrile: 0.1% formic acid in water (95:5, v/v) pumped through an Acquity UPLC BEH shield RP C18 column (1.7  $\mu\text{m}$ , 2.1  $\times$  150 mm) at a flow rate of 0.25 mL/min. The cone voltage was set at +40 V and the collision energy was set at 30 V with 0.04s dwell time of all drugs. Elemental Microanalyses were carried out at the Regional Center for Mycology and Biotechnology, Al-Azhar University. IR spectra (KBr disc) were recorded on a Shimadzu FT-IR 8400S infrared spectrophotometer. NMR spectra were recorded on a Bruker Ascend 400/R ( $^1\text{H}$ : 400,  $^{13}\text{C}$ : 100 MHz) spectrometer. The spectra were run at 400 MHz in deuterated dimethylsulfoxide (DMSO-*d*6). Chemical shifts were expressed in  $\delta$  units relative to TMS signal. Chemical shifts of exchangeable protons were characterized in D<sub>2</sub>O solution. All coupling constant (J) values are given in hertz. 6-(Un)substituted 2-aminobenzothiazoles **2a,b,e,h,j**, **5a-c** and **7** were purchased from Sigma-Aldrich, Germany and Alfa Aesar, Great Britain while **2c,d,f,g,i** were prepared according to the reported procedures [56–59].

#### 4.1.1 General procedure for the preparation of 3-(cyclopropylmethoxy)-4-(difluoromethoxy)-N-(substituted benzo[d]thiazol-2-yl)benzamide **4a-j**.

3-(cyclopropylmethoxy)-4-(difluoromethoxy)benzoic acid **3** (2 mmol., 0.52 gm) was refluxed with thionyl chloride (10 mL) for 1 hr. Excess thionyl chloride was distilled off and then the residue was washed with dry benzene followed by distillation (3x5 mL). The residue was dissolved in dry benzene and the reaction was stirred on hot followed by the addition of a solution of (un)substituted 2-aminobenzothiazole **2a-j** (2 mmol.) in dry benzene (10 mL) and anhydrous potassium carbonate (2 mmol., 0.28 gm). The reaction mixture was refluxed for 6 hr, filtered while hot and then concentrated. The precipitate obtained on cooling was filtered and recrystallized from ethanol.

#### 4.1.1.1 *N*-(benzo[d]thiazol-2-yl)-3-(cyclopropylmethoxy)-4-(difluoromethoxy)benzamide **4a**.

Obtained from the reaction of **2a** with **3**, white solid, yield 85 % (0.64 gm), mp 98-99° C. <sup>1</sup>HNMR (400 MHz, DMSO-*d*<sub>6</sub>) δ 12.45 (s, 1H, NH exchanged with D<sub>2</sub>O), 8.02 (dd, *J* = 2.28, 7.76, 1H, Ar H), 7.93 (dd, *J* = 1.80, 8.44, 1H, Ar H), 7.76-7.79 (m, 2H, Ar H), 7.47 (dd, *J* = 8.04, 1.24, 1H, Ar H), 7.34 (m, 2H, Ar H), 7.26 (s, 1H, CHF<sub>2</sub>), 4.02 (d, *J* = 7.00, 2H, CH<sub>2</sub>), 1.31 (m, 1H, CH), 0.62 (m, 2H, 2CH), 0.41 (m, 2H, 2CH). <sup>13</sup>C NMR (100 MHz, DMSO-*d*<sub>6</sub>) δ 172.48, 165.31, 159.45, 149.91, 148.65, 143.74, 131.93, 129.93, 126.64, 124.16, 122.18, 120.59, 119.44, 116.87, 114.37, 114.30, 73.86, 10.38, 3.52. IR (KBr) ν<sub>max</sub>/cm<sup>-1</sup>: 3394 (NH), 1651 (C=O). Elemental analysis calcd (%) for C<sub>19</sub>H<sub>16</sub>F<sub>2</sub>N<sub>2</sub>O<sub>3</sub>S (390.40): C, 58.45; H, 4.13; N, 7.18. Found: C, 58.79; H, 4.21; N, 7.43.

#### 4.1.1.2 3-(cyclopropylmethoxy)-4-(difluoromethoxy)-*N*-(4-methoxybenzo[d]thiazol-2-yl)benzamide **4b**.

Obtained from the reaction of **2b** with **3**, buff solid, yield 89 % (0.72 gm), mp 132-133° C. <sup>1</sup>HNMR (400 MHz, DMSO-*d*<sub>6</sub>) δ 13.00 (s, 1H, NH exchanged with D<sub>2</sub>O), 7.96 (d, *J* = 1.8, 1H, Ar H), 7.78(dd, *J* = 1.8, 8.40, 1H, Ar H), 7.57 (dd, , *J* = 1.96, 8.36, 1H, Ar H), 7.35 (d, *J* = 8.36, 1H, Ar H), 7.29 (d, *J* = 8.40, 1H, Ar H), 7.22 (s, 1H, CHF<sub>2</sub>), 7.02 (d, *J* = 8.2, 1H, Ar H), 4.01 (d, , *J* = 7.00, 2H, CH<sub>2</sub>), 3.94 (s, 3H, CH<sub>3</sub>), 1.30 (m, 1H, CH), 0.61 (m, 2H, 2 CH), 0.39 (m, 2H, 2 CH). <sup>13</sup>C NMR (100 MHz, DMSO-*d*<sub>6</sub>) δ 166.98, 164.92, 157.66, 152.36, 149.91, 143.75, 138.85, 129.75, 125.17, 120.60, 119.45, 115.19, 114.31, 113.88, 107.92, 73.72, 56.31, 10.38, 3.52. IR (KBr) ν<sub>max</sub>/cm<sup>-1</sup>: 3487 (NH) 1670 (C=O). Elemental analysis calcd (%) for C<sub>20</sub>H<sub>18</sub>F<sub>2</sub>N<sub>2</sub>O<sub>4</sub>S (420.43): C, 57.14; H, 4.32; N, 6.66. Found: C, 56.88; H, 4.43; N, 6.87.

4.1.1.3 3-(cyclopropylmethoxy)-4-(difluoromethoxy)-N-(6-methoxybenzo[d]thiazol-2-yl)benzamide **4c**.

Obtained from the reaction of **2c** with **3**, yellow solid, yield 45 % (0.37 gm), mp 122-123° C. <sup>1</sup>HNMR (500 MHz, DMSO-d<sub>6</sub>) δ 9.93 (s, 1H, NH exchanged with D<sub>2</sub>O), 7.52 (dd, *J* = 1.96, 8.36, 1H, Ar H), 7.49 (d, *J* = 1.92, 1H, Ar H), 7.32 (d, *J* = 8.24, 1H, Ar H), 7.30 (d, *J* = 1.84, 1H, Ar H), 7.08 (s, 1H, CHF<sub>2</sub>), 3.75 (s, 3H, CH<sub>3</sub>), 7.02 (d, *J* = 8.16, 1H, Ar H), 6.90 (dd, *J* = 1.8, 8.2, 1H, Ar H), 4.20 (s, 3H, OCH<sub>3</sub>), 3.86 (d, *J* = 6.96, 2H, CH<sub>2</sub>), 1.00 (m, 1H, CH), 0.33 (m, 2H, 2 CH), 0.12 (m, 2H, 2 CH). <sup>13</sup>C NMR (125 MHz, DMSO-d<sub>6</sub>) δ 166.95, 161.95, 150.19, 149.88, 145.63, 143.83, 129.11, 125.95, 124.36, 122.76, 120.58, 116.89, 115.96, 115.19, 114.32, 73.59, 55.50, 10.37, 3.48. IR (KBr) ν<sub>max</sub>\cm<sup>-1</sup>: 3417 (NH), 1670 (C=O). Elemental analysis calcd (%) for C<sub>20</sub>H<sub>18</sub>F<sub>2</sub>N<sub>2</sub>O<sub>4</sub>S (420.43): C, 57.14; H, 4.32; N, 6.66. Found: C, 56.88; H, 4.43; N, 6.87.

4.1.1.4 3-(cyclopropylmethoxy)-4-(difluoromethoxy)-N-(5,6-dimethoxybenzo[d]thiazol-2-yl)benzamide **4d**.

Obtained from the reaction of **2d** with **3**, yellow solid, yield 82 % (072 gm), mp 155-156° C. <sup>1</sup>HNMR (400 MHz, DMSO-d<sub>6</sub>) δ 9.97 (s, 1H, NH exchanged with D<sub>2</sub>O), 7.72 (s, 1H, Ar H), 7.62 (d, *J* = 1.8, 8.2, 1H, Ar H), 7.40 (s, 1H, Ar H), 7.31 (d, *J* = 1.8, 1H, Ar H), 7.22 (d, *J* = 8.2, 1H, Ar H), 7.02 (s, 1H, CHF<sub>2</sub>), 3.98 (d, *J* = 6.92, 2H, CH<sub>2</sub>), 3.81 (s, 3H, OCH<sub>3</sub>), 3.76 (s, 3H, OCH<sub>3</sub>), 1.30 (m, 1H, CH), 0.61 (m, 2H, 2 CH), 0.38 (m, 2H, 2 CH). <sup>13</sup>C NMR (100 MHz, DMSO-d<sub>6</sub>) δ 164.80, 149.97, 148.64, 148.45, 142.84, 132.44, 129.51, 120.94, 119.56, 116.99, 115.45, 114.42, 114.03, 113.10, 111.59, 73.72, 56.50, 56.31, 10.43, 3.52. IR (KBr) ν<sub>max</sub>\cm<sup>-1</sup>: 3259 (NH), 1647 (C=O). Elemental analysis calcd (%) for C<sub>21</sub>H<sub>20</sub>F<sub>2</sub>N<sub>2</sub>O<sub>5</sub>S (450.46): C, 55.99; H, 4.48; N, 6.22. Found: C, 56.23; H, 4.62; N, 6.39.

4.1.1.5 3-(cyclopropylmethoxy)-4-(difluoromethoxy)-N-(6-ethoxybenzo[d]thiazol-2-yl)benzamide **4e**.

Obtained from the reaction of **2e** with **3**, yellow solid, yield 74 % (0.62 gm), mp 255-256 °C. <sup>1</sup>H NMR (400 MHz, DMSO-*d*<sub>6</sub>) δ 10.11 (s, 1H, NH exchanged with D<sub>2</sub>O), 7.91 (d, *J* = 1.64, 1H, Ar H), 7.75 (dd, *J* = 1.68, 8.44, 1H, Ar H), 7.54 (d, *J* = 2.16, 1H, Ar H), 7.47 (d, *J* = 8.84, 1H, Ar H), 7.34 (d, *J* = 8.60, 1H, Ar H), 7.28 (s, 1H, CHF<sub>2</sub>), 7.00 (dd, *J* = 2.20, 8.84, 1H, Ar H), 4.08 (d, *J* = 6.92, 2H, CH<sub>2</sub>), 4.02 (q, *J* = 6.84, 2H, CH<sub>2</sub>CH<sub>3</sub>), 1.35 (t, *J* = 6.84, 3H, CH<sub>2</sub>CH<sub>3</sub>), 1.32 (m, 1H, CH), 0.60 (m, 2H, 2 CH), 0.38 (m, 2H, 2 CH). <sup>13</sup>C NMR (100 MHz, DMSO-*d*<sub>6</sub>) δ 168.63, 156.00, 149.86, 133.2, 132.28, 128.8, 125.47, 122.00, 120.56, 115.90, 115.61, 115.20, 114.40, 108.53, 105.79, 73.85, 64.27, 15.04, 10.39, 3.55. IR (KBr) ν<sub>max</sub>/cm<sup>-1</sup>: 3410 (NH), 1643 (C=O). Elemental analysis calcd (%) for C<sub>21</sub>H<sub>20</sub>F<sub>2</sub>N<sub>2</sub>O<sub>4</sub>S (434.46): C, 58.06; H, 4.64; N, 6.45. Found: C, 56.88; H, 4.43; N, 6.87.

4.1.1.6 3-(cyclopropylmethoxy)-4-(difluoromethoxy)-N-(6-fluorobenzo[d]thiazol-2-yl)benzamide **4f**.

Obtained from the reaction of **2f** with **3**, white solid, yield 45 % (0.36 gm), mp 155-156 °C. <sup>1</sup>H NMR (400 MHz, DMSO-*d*<sub>6</sub>) δ 7.84 (s, 1H, NH exchanged with D<sub>2</sub>O), 7.44 (d, *J* = 1.8, 1H, Ar H), 7.33 (dd, *J* = 1.88, 8.36, 1H, Ar H), 7.25 (d, *J* = 8.2, 1H, Ar H), 7.18 (s, 1H, CHF<sub>2</sub>), 7.06 (d, *J* = 8.32, 1H, Ar H), 7.00 (d, *J* = 8.2, 1H, Ar H), 6.81 (d, *J* = 8.2, 1H, Ar H), 3.77 (d, *J* = 6.96, 2H, CH<sub>2</sub>), 0.98 (m, 1H, CH), 0.44 (m, 2H, 2 CH), 0.22 (m, 2H, 2 CH). <sup>13</sup>C NMR (100 MHz, DMSO-*d*<sub>6</sub>) δ 167.34, 149.83, 142.53, 142.50, 142.47, 132.72, 120.70, 120.61, 119.56, 116.99, 114.43, 113.98, 73.61, 10.40, 3.47. IR (KBr) ν<sub>max</sub>/cm<sup>-1</sup>: 3371 (NH), 1651 (C=O). Elemental analysis calcd (%) for C<sub>19</sub>H<sub>15</sub>F<sub>3</sub>N<sub>2</sub>O<sub>3</sub>S (408.40): C, 55.88; H, 3.70; N, 6.86. Found: C, 55.98; H, 3.69; N, 6.98.

4.1.1.7 *N*-(6-chlorobenzo[*d*]thiazol-2-yl)-3-(cyclopropylmethoxy)-4-(difluoromethoxy)benzamide **4g**.

Obtained from the reaction of **2g** with **3**, yellow solid, yield 35 % (0.29 gm), mp 168-169 °C. <sup>1</sup>HNMR (400 MHz, DMSO-*d*<sub>6</sub>) δ 12.90 (s, 1H, NH exchanged with D<sub>2</sub>O), 7.59 (d, *J* = 8.2, 1H, Ar H), 7.40 (m, 2H, Ar H), 7.22 (d, *J* = 8.18, 1H, Ar H), 7.15 (s, 1H, CHF<sub>2</sub>), 7.10 (d, *J* = 1.8, 1H, Ar H), 7.04 (d, *J* = 1.8, 1H, Ar H), 3.80 (d, *J* = 6.88, 2H, CH<sub>2</sub>), 1.08 (m, 1H, CH), 0.42 (m, 2H, 2 CH), 0.20 (m, 2H, 2 CH). <sup>13</sup>C NMR (100 MHz, DMSO-*d*<sub>6</sub>) δ 166.98, 161.96, 149.88, 145.63, 143.84, 129.10, 125.96, 124.37, 122.77, 120.59, 119.47, 116.72, 115.97, 115.19, 114.14, 73.59, 10.38, 3.54. IR (KBr)  $\nu_{\max}$ /cm<sup>-1</sup>: 3417 (NH), 1680 (C=O). Elemental analysis calcd (%) for C<sub>19</sub>H<sub>15</sub>ClF<sub>2</sub>N<sub>2</sub>O<sub>3</sub>S (424.85): C, 53.72; H, 3.56; N, 6.59. Found: C, 53.98; H, 3.67; N, 6.89.

4.1.1.8 3-(cyclopropylmethoxy)-4-(difluoromethoxy)-*N*-(6-(trifluoromethyl)benzo[*d*]thiazol-2-yl)benzamide **4h**.

Obtained from the reaction of **2h** with **3**, white solid, yield 72 % (0.64 gm), mp 160-161 °C. <sup>1</sup>HNMR (400 MHz, DMSO-*d*<sub>6</sub>) δ 10.34 (s, 1H, NH exchanged with D<sub>2</sub>O), 7.74 (m, 1H, Ar H), 7.54 (m, 1H, Ar H), 7.39 (s, 1H, CHF<sub>2</sub>), 7.26 (d, *J* = 8.16, 1H, Ar H), 7.19 (d, *J* = 8.48, 1H, Ar H), 3.93 (d, *J* = 6.92, 2H, CH<sub>2</sub>), 1.23 (m, 1H, CH), 0.55 (m, 2H, 2 CH), 0.36 (m, 2H, 2 CH). <sup>13</sup>C NMR (100 MHz, DMSO-*d*<sub>6</sub>) δ 170.53, 166.92, 149.86, 143.82, 133.98, 130.29, 129.11, 128.75, 126.10, 124.84, 122.75, 120.56, 119.44, 116.88, 115.18, 114.31, 73.58, 10.36, 3.48. IR (KBr)  $\nu_{\max}$ /cm<sup>-1</sup>: 3294 (NH), 1654 (C=O). Elemental analysis calcd (%) for C<sub>20</sub>H<sub>15</sub>F<sub>5</sub>N<sub>2</sub>O<sub>3</sub>S (458.40): C, 52.40; H, 3.30; N, 6.11. Found: C, 52.67; H, 3.67; N, 6.39.

4.1.1.9 *N*-(6-cyanobenzo[*d*]thiazol-2-yl)-3-(cyclopropylmethoxy)-4-(difluoromethoxy)benzamide **4i**.

Obtained from the reaction of **2i** with **3**, yellow solid, yield 55 % (0.44 gm), mp 140-141 °C. <sup>1</sup>HNMR (400 MHz, DMSO-*d*<sub>6</sub>) δ 10.06 (s, 1H, NH exchanged with D<sub>2</sub>O), 7.50 (d, *J* = 1.88, 1H,

Ar H), 7.33 (m, 2H, Ar H), 7.16 (dd,  $J = 1.92, 8.2$ , 1H, Ar H), 7.07 (s, 1H, CHF<sub>2</sub>), 7.02 (d,  $J = 1.9$ , 1H, Ar H), 6.93 (d,  $J = 8.2$ , 1H, Ar H), 3.75 (d,  $J = 6.96$ , 2H, CH<sub>2</sub>), 1.02 (m, 1H, CH), 0.34 (m, 2H, 2 CH), 0.13 (m, 2H, 2 CH). <sup>13</sup>C NMR (100 MHz, DMSO-*d*<sub>6</sub>)  $\delta$  166.99, 161.92, 150.19, 148.80, 145.66, 143.84, 142.64, 130.29, 129.12, 125.97, 124.33, 122.76, 121.08, 120.58, 116.83, 115.19, 73.59, 10.28, 3.50. IR (KBr)  $\nu_{\max}$ /cm<sup>-1</sup>: 3377 (NH), 2233 (C≡N), 1671 (C=O). Elemental analysis calcd (%) for C<sub>20</sub>H<sub>15</sub>F<sub>2</sub>N<sub>3</sub>O<sub>3</sub>S (415.41): C, 57.83; H, 3.64; N, 10.12. Found: C, 58.07; H, 3.72; N, 10.34.

#### 4.1.1.10 3-(cyclopropylmethoxy)-4-(difluoromethoxy)-N-(6-nitrobenzo[d]thiazol-2-yl)benzamide **4j**.

Obtained from the reaction of **2j** with **3**, yellow solid, yield 76 % (0.64 gm), mp 144-145°C. <sup>1</sup>H NMR (400 MHz, DMSO-*d*<sub>6</sub>)  $\delta$  9.62 (s, 1H, NH exchanged with D<sub>2</sub>O), 8.80 (d,  $J = 2.44$ , 1H, Ar H), 8.27 (dd,  $J = 2.4, 8.92$ , 1H, Ar H), 8.19 (d,  $J = 8.88$ , 1H, Ar H), 7.91 (dd,  $J = 1.88, 8.92$ , 1H, Ar H), 7.76 (d,  $J = 1.84$ , 1H, Ar H), 7.57 (d,  $J = 8.92$ , 1H, Ar H), 7.53 (s, 1H, CHF<sub>2</sub>), 4.03 (d,  $J = 7$ , 2H, CH<sub>2</sub>), 1.19 (m, 1H, CH), 0.59 (m, 2H, 2CH), 0.37 (m, 2H, 2CH). <sup>13</sup>C NMR (100 MHz, DMSO-*d*<sub>6</sub>)  $\delta$  171.78, 164.81, 150.44, 149.86, 142.69, 132.68, 129.27, 128.61, 123.23, 122.74, 120.89, 119.31, 116.83, 115.77, 114.49, 73.89, 10.37, 3.55. IR (KBr)  $\nu_{\max}$ /cm<sup>-1</sup>: 3282 (NH), 1651 (C=O), 1527 & 1342 (NO<sub>2</sub>). Elemental analysis calcd (%) for C<sub>19</sub>H<sub>15</sub>F<sub>2</sub>N<sub>3</sub>O<sub>5</sub>S (435.40): C, 52.41; H, 3.47; N, 9.65. Found: C, 52.68; H, 3.60; N, 9.84.

#### 4.1.1.11 N-(benzo[d]thiazol-6-yl)-3-(cyclopropylmethoxy)-4-(difluoromethoxy)benzamide **6a**.

Obtained from the reaction of **5a** with **3**, white solid, yield 85 % (0.64 gm), mp 95-96°C. <sup>1</sup>H NMR (400 MHz, DMSO-*d*<sub>6</sub>)  $\delta$  10.48 (s, 1H, NH exchanged with D<sub>2</sub>O), 9.31 (s, 1H, Ar H), 8.65 (d,  $J = 1.88$ , 1H, Ar H), 8.08 (d,  $J = 8.80$ , 1H, Ar H), 7.82 (dd,  $J = 1.90, 8.84$ , 1H, Ar H), 7.69 (d,  $J = 1.8$ , 1H, Ar H), 7.63 (dd,  $J = 1.8, 8.36$ , 1H, Ar H), 7.34 (d,  $J = 8.32$ , 1H, Ar H), 7.23

(s, 1H,  $\text{CHF}_2$ ), 4.01 (d,  $J = 6.96$ , 2H,  $\text{CH}_2$ ), 1.30 (m, 1H, CH), 0.61 (m, 2H, 2CH), 0.39 (m, 2H, 2CH).  $^{13}\text{C}$  NMR (100 MHz, DMSO- $d_6$ )  $\delta$  165.15, 155.49, 149.99, 142.85, 137.15, 134.55, 133.14, 123.29, 121.04, 120.78, 120.55, 119.53, 116.97, 114.23, 113.65, 73.78, 10.43, 3.52. IR (KBr)  $\nu_{\text{max}}\text{cm}^{-1}$ : 3271 (NH), 1651 (C=O). Elemental analysis calcd (%) for  $\text{C}_{19}\text{H}_{16}\text{F}_2\text{N}_2\text{O}_3\text{S}$  (390.40): C, 58.45; H, 4.13; N, 7.18. Found: C, 58.68; H, 4.03; N, 7.47.

#### 4.1.1.12 3-(cyclopropylmethoxy)-4-(difluoromethoxy)-N-(2-methylbenzo[d]thiazol-6-yl)benzamide **6b**.

Obtained from the reaction of **5b** with **3**, brown solid, yield 72 % (0.56 gm), mp 122-123°C.  $^1\text{H}$ NMR (400 MHz, DMSO- $d_6$ )  $\delta$  10.42 (s, 1H, NH exchanged with  $\text{D}_2\text{O}$ ), 8.50 (d,  $J = 1.98$ , 1H, Ar H), 7.89 (d,  $J = 8.80$ , 1H, Ar H), 7.75 (dd,  $J = 2.00$ , 8.76, 1H, Ar H), 7.69 (d,  $J = 1.88$ , 1H, Ar H), 7.63 (dd,  $J = 1.88$ , 8.32, 1H, Ar H), 7.34 (d,  $J = 8.3$ , 1H, Ar H), 7.22 (s, 1H,  $\text{CHF}_2$ ), 4.00 (d,  $J = 7$ , 2H,  $\text{CH}_2$ ), 2.78 (s, 3H,  $\text{CH}_3$ ), 1.28 (m, 1H, CH), 0.61 (m, 2H, 2CH), 0.39 (m, 2H, 2CH).  $^{13}\text{C}$  NMR (100 MHz, DMSO- $d_6$ )  $\delta$  166.35, 165.05, 149.97, 149.88, 142.80, 136.45, 136.06, 133.18, 122.17, 121.01, 120.77, 119.53, 116.96, 114.19, 113.43, 73.77, 20.12, 10.43, 3.52. IR (KBr)  $\nu_{\text{max}}\text{cm}^{-1}$ : 3298 (NH), 1670 (C=O). Elemental analysis calcd (%) for  $\text{C}_{20}\text{H}_{18}\text{F}_2\text{N}_2\text{O}_3\text{S}$  (404.43): C, 59.40; H, 4.49; N, 6.93. Found: C, 59.23; H, 4.68; N, 7.08.

#### 4.1.1.13 3-(cyclopropylmethoxy)-4-(difluoromethoxy)-N-(2-mercaptobenzo[d]thiazol-6-yl)benzamide **6c**.

Obtained from the reaction of **5c** with **3**, yellow solid, yield 82 % (0.67 gm), mp 210-211°C.  $^1\text{H}$ NMR (400 MHz, DMSO- $d_6$ )  $\delta$  12.15 (s, 1H, SH exchanged with  $\text{D}_2\text{O}$ ), 10.53 (s, 1H, NH exchanged with  $\text{D}_2\text{O}$ ), 7.83 (d,  $J = 1.62$ , 1H, Ar H), 7.65 (m, 2H, Ar H), 7.33 (3, 2H, Ar H), 7.2 (m, 2H, Ar H,  $\text{CHF}_2$ ), 4.00 (d,  $J = 6.2$ , 2H,  $\text{CH}_2$ ), 1.28 (m, 1H, CH), 0.58 (m, 2H, 2CH), 0.37 (m, 2H, 2CH).  $^{13}\text{C}$  NMR (100 MHz, DMSO- $d_6$ )  $\delta$  190.22, 164.91, 150.05, 149.70, 139.78, 136.2,

132.96, 131.77, 131.06, 123.51, 121.4, 117.07, 115.12, 114.24, 113.89, 113.61, 73.85, 10.43, 3.53. IR (KBr)  $\nu_{\max}$ /cm<sup>-1</sup>: 3367 (NH), 2580 (SH), 1690 (C=O). Elemental analysis calcd (%) for C<sub>19</sub>H<sub>16</sub>F<sub>2</sub>N<sub>2</sub>O<sub>3</sub>S<sub>2</sub> (422.46): C, 54.02; H, 3.82; N, 6.63. Found: C, 53.89; H, 3.63; N, 6.92.

#### 4.1.1.14 3-(cyclopropylmethoxy)-4-(difluoromethoxy)-N-(thiazol-2-yl)benzamide **8**.

Obtained from the reaction of **7** with **3**, white solid, yield 55 % (0.36 gm), mp 97-98 °C. <sup>1</sup>H NMR (400 MHz, DMSO-*d*<sub>6</sub>)  $\delta$  12.85 (s, 1H, NH exchanged with D<sub>2</sub>O), 7.73 (d, *J* = 1.2, 1H, Ar H), 7.54 (m, 2H, Ar H), 7.37 (dd, *J* = 4.8 1H, Ar H), 7.23 (d, *J* = 8.12, 1H, Ar H), 7.18 (s, 1H, CHF<sub>2</sub>), 3.91 (d, , *J* = 6.88, 2H, CH<sub>2</sub>), 1.22 (m, 1H, CH), 0.55 (m, 2H, 2 CH), 0.34 (m, 2H, 2 CH). <sup>13</sup>C NMR (100 MHz, DMSO-*d*<sub>6</sub>)  $\delta$  166.87, 161.84, 149.83, 143.79, 133.89, 129.02, 122.73, 120.55, 119.39, 116.75, 115.16, 73.67, 10.24, 3.46. IR (KBr)  $\nu_{\max}$ /cm<sup>-1</sup>: 3336 (NH), 1697 (C=O). Elemental analysis calcd (%) for C<sub>15</sub>H<sub>14</sub>F<sub>2</sub>N<sub>2</sub>O<sub>3</sub>S (340.34): C, 52.94; H, 4.15; N, 8.23. Found: C, 53.08; H, 4.34; N, 8.52.

## 4.2 Biological evaluation.

PDE-4B enzymatic assay was performed for roflumilast and all the synthesized compounds using Human PDE4B ELISA Kit (MBS760982), BPS Bioscience®. PDE-4D enzymatic assay was performed for roflumilast, **4a**, **6a** and **6c** using Human PDE4D) ELISA Kit (MBS732623), BPS Bioscience®. Intracellular cAMP was measured for roflumilast, **4a**, and **6c** using ab133038-Direct cAMP ELISA Kit, Abcam®. The quantification of TNF- $\alpha$  was performed for roflumilast, **4a**, and **6c** using ab181421 –TNF-alpha Human SimpleStep® ELISA Kit obtained from Abcam®. Manufacturer's instructions were followed for each kit. Statistical significance between the obtained biological values of roflumilast and the tested compounds was calculated using one-way ANOVA followed by Bonferroni's multiple comparisons test (*p*<0.05). The tested compounds were examined for known classes of assay interference compounds. According to

SwissADME tool [69], none of the compounds contain substructural features recognized as pan assay interference compounds (PAINS).

#### 4.3 *Molecular docking study*

Molecular docking studies were carried out using Molecular Operating Environment (MOE, 10.2008) software. Minimization was performed with MOE until an RMSD gradient of 0.05 kcal·mol<sup>-1</sup> Å<sup>-1</sup> with MMFF94x force field and the partial charges were automatically calculated. The X-ray crystallographic structures of PDE-4B and PDE-4D co-crystallized with roflumilast as inhibitor were downloaded from the Protein Data Bank, <https://www.rcsb.org/>, (PDB ID: 1XMU and 1XOQ, respectively) [42]. Preparation of the enzymes for docking study was done by removing chain B of its dimer, ligands and water molecules that are not involved in the binding. The enzymes were then protonated using Protonate 3D protocol in MOE with default options. Triangle Matcher placement method and London dG scoring function were used for the docking protocol and forcefield was used as refinement. The co-crystallized ligand (roflumilast) was redocked into the active site of each enzyme for validation of the docking setup. Then, the binding mode and the binding interactions of the newly synthesized compounds at the active site of PDE-4B and PDE-4D were predicted by using the validated setup. Roflumilast was used as reference compound to compare its binding score to that of the newly synthesized compounds and so their affinity to the target enzymes (PDE4B and PDE4D).

#### 4.4 *Determination of in vivo pharmacokinetic parameters in rats*

Twenty-four male Sprague-Dawley rats (250-300 g), obtained from the Laboratory Animal Center, Faculty of Pharmacy, Cairo University, were placed in cages, six per cage and had free access to food and water. The temperature was set at 25°C and maintained in a 12 h light/dark cycle. The rats were randomly divided into four groups ( $n=6$ ): reference group (roflumilast) and

3 test groups (compounds **4a**, **6a** and **6c**). All experimental procedures were approved by and conducted in accordance with the institutional guidelines of the Institutional Review Board of Faculty of Pharmacy, Cairo University and the regulations of the local Animal Welfare authorities. Each group was dosed with a subcutaneous dose (1 mg/kg). The compounds were formulated in 5% tween 80 and normal saline. After single administration, blood samples were withdrawn at the following time intervals: 0.25, 0.5, 1, 2, 4, 6, 8 and 24 h. All blood samples were collected into heparinized tubes, centrifuged at 4000 rpm for 10 min at 4°C and subsequently stored at -20°C prior to analysis. Plasma samples were extracted then analyzed by a validated UPLC-MS/MS method for each individual compound. The pharmacokinetic parameters were calculated using WinNonlin Software. Statistical significance between the pharmacokinetic parameters ( $t_{1/2}$ ,  $C_{max}$ ,  $AUC_{0-t}$ ,  $AUC_{0-\infty}$ ,  $V_d$  and CL) of roflumilast and the tested compounds was calculated using one-way ANOVA followed by Bonferroni's multiple comparisons test ( $p < 0.05$ ).

#### 4.5 *In vitro* pharmacokinetic studies

##### 4.5.1 *Metabolic stability and metabolite identification in rat S9 fraction*

The assay was performed with Liver subcellular fraction (9,000× g S9 fraction) from male Wistar rats, prepared as previously described [70,71]. All steps were performed at 0–4°C with cold and sterile solutions and glassware. Compounds **4a**, **6a** and **6c** in addition to roflumilast were tested for their phase I metabolic stability. Twenty  $\mu$ M of each of the tested compounds was incubated with 1 mg/mL prepared pooled mammalian liver S9 fraction, 10 mM NADPH, 100 mM  $MgCl_2$  and 100 mM Tris buffer (pH 7.4) 37 °C for 0, 15, 30 and 60 min at a final volume of 0.5 mL (except for roflumilast which was incubated for time intervals 0, 5, 10, 15 and 30 min.). Reactions were terminated by protein precipitation using 0.5 mL cold acetonitrile and

20  $\mu$ L internal standard (chlorzoxazone). The samples were vortex mixed and centrifuged at 4000 rpm for 10 min at 4 °C. The samples were analyzed using a Younglin HPLC-UV Acme 9000 system (Korea) to determine the remained intact compound.

The metabolism of compounds **4a** and **6a** were further investigated to identify their possible metabolites by analyzing the samples after 60 min incubation with S9 fraction and NADPH using UPLC-MS/MS (Waters TQD LC-MS-MS system).

#### 4.5.2 Human plasma protein binding determination

Compounds **4a**, **6a**, **6c** and roflumilast were evaluated for their human plasma protein (VACSERA-EGYPT) binding (PPB) with an equilibrium dialysis device using a Dialysis cellulose membrane, Sigma-Aldrich, USA with a molecular weight cut-off of 12-14 KDa. The tested compounds were incubated with human plasma protein at 37°C for 5 hr then the concentration of each compound was estimated in plasma compartment and buffer compartment (isotonic phosphate-buffered saline (PBS), pH 7.4) using validated RP-HPLC-UV methods (Younglin instrument Acme 9000, Korea). The percentage of bound fraction was calculated by the following equation:

$$\{\% \text{ Bound} = 1 - (\text{Concentration in buffer} / \text{Concentration in plasma}) * 100\}$$

## 5 References

- [1] D.S. Postma, Remodeling in Asthma and Chronic Obstructive Pulmonary Disease, *Proc. Am. Thorac. Soc.* 3 (2006) 434–439. doi:10.1513/pats.200601-006AW.
- [2] K.F. Rabe, H. Watz, Chronic obstructive pulmonary disease., *Lancet* (London, England). 389 (2017) 1931–1940. doi:10.1016/S0140-6736(17)31222-9.
- [3] S.R. Rutgers, D.S. Postma, N.H. ten Hacken, H.F. Kauffman, T.W. van Der Mark, G.H. Koëter, W. Timens, Ongoing airway inflammation in patients with COPD who do not currently smoke., *Thorax*. 55 (2000) 12–8. doi:10.1136/THORAX.55.1.12.
- [4] P.J. Barnes, Cytokine modulators as novel therapies for airway disease., *Eur. Respir. J. Suppl.* 34 (2001) 67s–77s. <http://www.ncbi.nlm.nih.gov/pubmed/12392037> (accessed October 7, 2017).
- [5] P.J. Barnes, T.T. Hansel, Prospects for new drugs for chronic obstructive pulmonary disease, *Lancet*. 364 (2004) 985–996. doi:10.1016/S0140-6736(04)17025-6.
- [6] A. Alsaedi, D.D. Sin, F.A. McAlister, The effects of inhaled corticosteroids in chronic obstructive pulmonary disease: a systematic review of randomized placebo-controlled trials., *Am. J. Med.* 113 (2002) 59–65. <http://www.ncbi.nlm.nih.gov/pubmed/12106623> (accessed October 7, 2017).
- [7] R.A. Pauwels, C.-G. Löfdahl, L.A. Laitinen, J.P. Schouten, D.S. Postma, N.B. Pride, S. V. Ohlsson, Long-Term Treatment with Inhaled Budesonide in Persons with Mild Chronic Obstructive Pulmonary Disease Who Continue Smoking, *N. Engl. J. Med.* 340 (1999) 1948–1953. doi:10.1056/NEJM199906243402503.

- [8] P.S. Burge, P.M. Calverley, P.W. Jones, S. Spencer, J.A. Anderson, T.K. Maslen, Randomised, double blind, placebo controlled study of fluticasone propionate in patients with moderate to severe chronic obstructive pulmonary disease: the ISOLDE trial., *BMJ*. 320 (2000) 1297–303. doi:10.1136/BMJ.320.7245.1297.
- [9] R. Wise, J. Connett, G. Weinmann, P. Scanlon, M. Skeans, Effect of Inhaled Triamcinolone on the Decline in Pulmonary Function in Chronic Obstructive Pulmonary Disease, *N. Engl. J. Med.* 343 (2000) 1902–1909. doi:10.1056/NEJM200012283432601.
- [10] M. Ichinose, H. Sugiura, S. Yamagata, A. Koarai, K. Shirato, Increase in Reactive Nitrogen Species Production in Chronic Obstructive Pulmonary Disease Airways, *Am. J. Respir. Crit. Care Med.* 162 (2000) 701–706. doi:10.1164/ajrccm.162.2.9908132.
- [11] A.T. Hill, D. Bayley, R.A. Stockley, The Interrelationship of Sputum Inflammatory Markers in Patients with Chronic Bronchitis, *Am. J. Respir. Crit. Care Med.* 160 (1999) 893–898. doi:10.1164/ajrccm.160.3.9901091.
- [12] P. Montuschi, S.A. Kharitonov, G. Ciabattini, P.J. Barnes, Exhaled leukotrienes and prostaglandins in COPD., *Thorax*. 58 (2003) 585–8. <http://www.ncbi.nlm.nih.gov/pubmed/12832671> (accessed October 7, 2017).
- [13] K.L. Davenpeck, K.L. Berens, R.A. Dixon, B. Dupre, B.S. Bochner, Inhibition of adhesion of human neutrophils and eosinophils to P-selectin by the sialyl Lewis antagonist TBC1269: preferential activity against neutrophil adhesion in vitro., *J. Allergy Clin. Immunol.* 105 (2000) 769–75. <http://www.ncbi.nlm.nih.gov/pubmed/10756228> (accessed October 7, 2017).

- [14] D.W. Hay, H.M. Sarau, Interleukin-8 receptor antagonists in pulmonary diseases., *Curr. Opin. Pharmacol.* 1 (2001) 242–7. <http://www.ncbi.nlm.nih.gov/pubmed/11712746> (accessed October 7, 2017).
- [15] M.H. Rabinowitz, R.C. Andrews, J.D. Becherer, D.M. Bickett, D.G. Bubacz, J.G. Conway, D.J. Cowan, M. Gaul, K. Glennon, M.H. Lambert, M.A. Leesnitzer, D.L. McDougald, M.L. Moss, D.L. Musso, M.C. Rizzolio, Design of selective and soluble inhibitors of tumor necrosis factor- $\alpha$  converting enzyme (TACE), *J. Med. Chem.* 44 (2001) 4252–4267. doi:10.1021/jm0102654.
- [16] A.C. Castro, L.C. Dang, F. Soucy, L. Grenier, H. Mazdiyasni, M. Hottelet, L. Parent, C. Pien, V. Palombella, J. Adams, Novel IKK inhibitors: beta-carbolines., *Bioorg. Med. Chem. Lett.* 13 (2003) 2419–22. <http://www.ncbi.nlm.nih.gov/pubmed/12824047> (accessed October 7, 2017).
- [17] D.C. Underwood, R.R. Osborn, S. Bochnowicz, E.F. Webb, D.J. Rieman, J.C. Lee, A.M. Romanic, J.L. Adams, D.W. Hay, D.E. Griswold, SB 239063, a p38 MAPK inhibitor, reduces neutrophilia, inflammatory cytokines, MMP-9, and fibrosis in lung., *Am. J. Physiol. Lung Cell. Mol. Physiol.* 279 (2000) L895-902. <http://www.ncbi.nlm.nih.gov/pubmed/11053025> (accessed October 7, 2017).
- [18] S. Ward, Y. Sotsios, J. Dowden, I. Bruce, P. Finan, Therapeutic potential of phosphoinositide 3-kinase inhibitors., *Chem. Biol.* 10 (2003) 207–13. <http://www.ncbi.nlm.nih.gov/pubmed/12670534> (accessed October 7, 2017).
- [19] B. Seed, C. Jiang, A.T. Ting, PPAR-gamma agonists inhibit production of monocyte

- inflammatory cytokines., *Nature*. 391 (1998) 82–86. doi:10.1038/34184.
- [20] H.J. Patel, M.G. Belvisi, D. Bishop-Bailey, M.H. Yacoub, J.A. Mitchell, Activation of peroxisome proliferator-activated receptors in human airway smooth muscle cells has a superior anti-inflammatory profile to corticosteroids: relevance for chronic obstructive pulmonary disease therapy., *J. Immunol.* 170 (2003) 2663–9. doi:10.4049/JIMMUNOL.170.5.2663.
- [21] S.G. Harris, R.P. Phipps, induction of apoptosis in mouse t cells upon peroxisome proliferator-activated receptor gamma (ppar- $\gamma$ ) binding, in: Springer, Boston, MA, 2002: pp. 421–425. doi:10.1007/978-1-4615-0193-0\_65.
- [22] G. Sturton, M. Fitzgerald, Phosphodiesterase 4 inhibitors for the treatment of COPD., *Chest*. 121 (2002) 192S–196S. <http://www.ncbi.nlm.nih.gov/pubmed/12010850> (accessed October 8, 2017).
- [23] V. Boswell-Smith, D. Spina, C.P. Page, Phosphodiesterase inhibitors, *Br. J. Pharmacol.* 147 (2009) S252–S257. doi:10.1038/sj.bjp.0706495.
- [24] D.M.G. Halpin, ABCD of the phosphodiesterase family: interaction and differential activity in COPD., *Int. J. Chron. Obstruct. Pulmon. Dis.* 3 (2008) 543–61. <http://www.ncbi.nlm.nih.gov/pubmed/19281073> (accessed October 31, 2017).
- [25] J.E. Souness, D. Aldous, C. Sargent, Immunosuppressive and anti-inflammatory effects of cyclic AMP phosphodiesterase (PDE) type 4 inhibitors., *Immunopharmacology*. 47 (2000) 127–62. <http://www.ncbi.nlm.nih.gov/pubmed/10878287> (accessed October 7, 2017).

- [26] M.A. Giembycz, Development status of second generation PDE4 inhibitors for asthma and COPD: the story so far., *Monaldi Arch. Chest Dis.* 57 (2002) 48–64. <http://www.ncbi.nlm.nih.gov/pubmed/12174704> (accessed October 7, 2017).
- [27] C.D. Nicholson, M. Shahid, Inhibitors of Cyclic Nucleotide Phosphodiesterase Isoenzymes—their Potential Utility in the Therapy of Asthma, *Pulm. Pharmacol.* 7 (1994) 7–17. doi:10.1006/PULP.1994.1001.
- [28] J.M. Palacios, J. Beleta, V. Segarra, Second messenger systems as targets for new therapeutic agents: focus on selective phosphodiesterase inhibitors., *Farmaco.* 50 (1995) 819–27. <http://www.ncbi.nlm.nih.gov/pubmed/8634072> (accessed October 7, 2017).
- [29] J. Westbrook, Z. Feng, S. Jain, T.N. Bhat, N. Thanki, V. Ravichandran, G.L. Gilliland, W. Bluhm, H. Weissig, D.S. Greer, P.E. Bourne, H.M. Berman, The Protein Data Bank: unifying the archive., *Nucleic Acids Res.* 30 (2002) 245–8. <http://www.ncbi.nlm.nih.gov/pubmed/11752306> (accessed October 7, 2017).
- [30] S.-L.C. Jin, M. Conti, Induction of the cyclic nucleotide phosphodiesterase PDE4B is essential for LPS-activated TNF- responses, *Proc. Natl. Acad. Sci.* 99 (2002) 7628–7633. doi:10.1073/pnas.122041599.
- [31] A. Robichaud, P.B. Stamatiou, S.-L.C. Jin, N. Lachance, D. MacDonald, F. Laliberté, S. Liu, Z. Huang, M. Conti, C.-C. Chan, Deletion of phosphodiesterase 4D in mice shortens alpha(2)-adrenoceptor-mediated anesthesia, a behavioral correlate of emesis., *J. Clin. Invest.* 110 (2002) 1045–52. doi:10.1172/JCI15506.
- [32] M. Ariga, B. Neitzert, S. Nakae, G. Mottin, C. Bertrand, M.P. Pruniaux, S.-L.C. Jin, M.

- Conti, Nonredundant function of phosphodiesterases 4D and 4B in neutrophil recruitment to the site of inflammation., *J. Immunol.* 173 (2004) 7531–8. <http://www.ncbi.nlm.nih.gov/pubmed/15585880> (accessed October 7, 2017).
- [33] A. Hatzelmann, C. Schudt, Anti-inflammatory and immunomodulatory potential of the novel PDE4 inhibitor roflumilast in vitro., *J. Pharmacol. Exp. Ther.* 297 (2001) 267–79. <http://www.ncbi.nlm.nih.gov/pubmed/11259554> (accessed October 30, 2017).
- [34] D.R. Gorja, S. Mukherjee, C.L.T. Meda, G.S. Deora, K. Lalith Kumar, A. Jain, G.H. Chaudhari, K.S. Chennubhotla, R.K. Banote, P. Kulkarni, K.V.L. Parsa, K. Mukkanti, M. Pal, Novel N-indolylmethyl substituted olanzapine derivatives: their design, synthesis and evaluation as PDE4B inhibitors, *Org. Biomol. Chem.* 11 (2013) 2075–2079. doi:10.1039/c3ob27424a.
- [35] K.F. Rabe, E.D. Bateman, D. O'Donnell, S. Witte, D. Bredenbröker, T.D. Bethke, Roflumilast—an oral anti-inflammatory treatment for chronic obstructive pulmonary disease: a randomised controlled trial, *Lancet.* 366 (2005) 563–571. doi:10.1016/S0140-6736(05)67100-0.
- [36] K.F. Rabe, Update on roflumilast, a phosphodiesterase 4 inhibitor for the treatment of chronic obstructive pulmonary disease, *Br. J. Pharmacol.* 163 (2011) 53–67. doi:10.1111/j.1476-5381.2011.01218.x.
- [37] G. Lahu, A. Huennemeyer, O. von Richter, R. Hermann, R. Herzog, N. McCracken, K. Zech, Effect of Single and Repeated Doses of Ketoconazole on the Pharmacokinetics of Roflumilast and Roflumilast N-Oxide, *J. Clin. Pharmacol.* 48 (2008) 1339–1349.

- doi:10.1177/0091270008321941.
- [38] O. Von Richter, G. Lahu, A. Huennemeyer, R. Herzog, K. Zech, R. Hermann, Effect of fluvoxamine on the pharmacokinetics of roflumilast and roflumilast N-oxide, *Clin. Pharmacokinet.* 46 (2007) 613–622. doi:10.2165/00003088-200746070-00006.
- [39] M.M. Cotreau, L.L. von Moltke, D.J. Greenblatt, The Influence of Age and Sex on the Clearance of Cytochrome P450 3A Substrates, *Clin. Pharmacokinet.* 44 (2005) 33–60. doi:10.2165/00003088-200544010-00002.
- [40] Z. Bebia, S. Buch, J. Wilson, R. Frye, M. Romkes, A. Cechetti, D. Chavesgnecco, R. Branch, Bioequivalence revisited: Influence of age and sex on CYP enzymes, *Clin. Pharmacol. Ther.* 76 (2004) 618–627. doi:10.1016/j.clpt.2004.08.021.
- [41] A.A. Mangoni, S.H.D. Jackson, Age-related changes in pharmacokinetics and pharmacodynamics: basic principles and practical applications., *Br. J. Clin. Pharmacol.* 57 (2004) 6–14. doi:10.1046/J.1365-2125.2003.02007.X.
- [42] G.L. Card, B.P. England, Y. Suzuki, D. Fong, B. Powell, B. Lee, C. Luu, M. Tabriziad, S. Gillette, P.N. Ibrahim, D.R. Artis, G. Bollag, M. V. Milburn, S.-H. Kim, J. Schlessinger, K.Y.J. Zhang, Structural Basis for the Activity of Drugs that Inhibit Phosphodiesterases, *Structure.* 12 (2004) 2233–2247. doi:10.1016/j.str.2004.10.004.
- [43] R.X. Xu, A.M. Hassell, D. Vanderwall, M.H. Lambert, W.D. Holmes, M.A. Luther, W.J. Rocque, M. V Milburn, Y. Zhao, H. Ke, R.T. Nolte, Atomic structure of PDE4: insights into phosphodiesterase mechanism and specificity., *Science.* 288 (2000) 1822–5. <http://www.ncbi.nlm.nih.gov/pubmed/10846163> (accessed October 8, 2017).

- [44] J.N. Hamblin, T.D.R. Angell, S.P. Ballantine, C.M. Cook, A.W.J. Cooper, J. Dawson, C.J. Delves, P.S. Jones, M. Lindvall, F.S. Lucas, C.J. Mitchell, M.Y. Neu, L.E. Ranshaw, Y.E. Solanke, D.O. Somers, J.O. Wiseman, Pyrazolopyridines as a novel structural class of potent and selective PDE4 inhibitors., *Bioorg. Med. Chem. Lett.* 18 (2008) 4237–41. doi:10.1016/j.bmcl.2008.05.052.
- [45] M.D. Woodrow, S.P. Ballantine, M.D. Barker, B.J. Clarke, J. Dawson, T.W. Dean, C.J. Delves, B. Evans, S.L. Gough, S.B. Guntrip, S. Holman, D.S. Holmes, M. Kranz, M.K. Lindvaal, F.S. Lucas, M. Neu, L.E. Ranshaw, Y.E. Solanke, D.O. Somers, P. Ward, J.O. Wiseman, Quinolines as a novel structural class of potent and selective PDE4 inhibitors. Optimisation for inhaled administration., *Bioorg. Med. Chem. Lett.* 19 (2009) 5261–5. doi:10.1016/j.bmcl.2009.04.012.
- [46] K.Y.J. Zhang, G.L. Card, Y. Suzuki, D.R. Artis, D. Fong, S. Gillette, D. Hsieh, J. Neiman, B.L. West, C. Zhang, M. V Milburn, S.-H. Kim, J. Schlessinger, G. Bollag, A glutamine switch mechanism for nucleotide selectivity by phosphodiesterases., *Mol. Cell.* 15 (2004) 279–86. doi:10.1016/j.molcel.2004.07.005.
- [47] C.J. Mitchell, S.P. Ballantine, D.M. Coe, C.M. Cook, C.J. Delves, M.D. Dowle, C.D. Edlin, J.N. Hamblin, S. Holman, M.R. Johnson, P.S. Jones, S.E. Keeling, M. Kranz, M. Lindvall, F.S. Lucas, M. Neu, Y.E. Solanke, D.O. Somers, N.A. Trivedi, J.O. Wiseman, Pyrazolopyridines as potent PDE4B inhibitors: 5-heterocycle SAR., *Bioorg. Med. Chem. Lett.* 20 (2010) 5803–6. doi:10.1016/j.bmcl.2010.07.136.
- [48] J. Taltavull, J. Serrat, J. Gràcia, A. Gavaldà, M. Andrés, M. Córdoba, M. Miralpeix, D. Vilella, J. Beleta, H. Ryder, L. Pagès, Synthesis and Biological Activity of

- Pyrido[3',2':4,5]thieno[3,2-*d*]pyrimidines as Phosphodiesterase Type 4 Inhibitors, *J. Med. Chem.* 53 (2010) 6912–6922. doi:10.1021/jm100524j.
- [49] K. Kagayama, T. Morimoto, S. Nagata, F. Katoh, X. Zhang, N. Inoue, A. Hashino, K. Kageyama, J. Shikaura, T. Niwa, Synthesis and biological evaluation of novel phthalazinone derivatives as topically active phosphodiesterase 4 inhibitors, *Bioorg. Med. Chem.* 17 (2009) 6959–6970. doi:10.1016/j.bmc.2009.08.014.
- [50] K. Ochiai, S. Takita, T. Eiraku, A. Kojima, K. Iwase, T. Kishi, K. Fukuchi, T. Yasue, D.R. Adams, R.W. Allcock, Z. Jiang, Y. Kohno, Phosphodiesterase inhibitors. Part 3: Design, synthesis and structure-activity relationships of dual PDE3/4-inhibitory fused bicyclic heteroaromatic-dihydropyridazinones with anti-inflammatory and bronchodilatory activity, *Bioorganic Med. Chem.* 20 (2012) 1644–1658. doi:10.1016/j.bmc.2012.01.033.
- [51] C. Brullo, M. Massa, M. Rocca, C. Rotolo, S. Guariento, D. Rivera, R. Ricciarelli, E. Fedele, P. Fossa, O. Bruno, Synthesis, Biological Evaluation, and Molecular Modeling of New 3-(Cyclopentyloxy)-4-methoxybenzaldehyde *O* -(2-(2,6-Dimethylmorpholino)-2-oxoethyl) Oxime (GEBR-7b) Related Phosphodiesterase 4D (PDE4D) Inhibitors, *J. Med. Chem.* 57 (2014) 7061–7072. doi:10.1021/jm500855w.
- [52] S.S. Laddha, S.G. Wadodkar, S.K. Meghal, cAMP-dependent phosphodiesterase inhibition and SAR studies on novel 6,8-disubstituted 2-phenyl-3-(substituted benzothiazole-2-yl)-4[3H]-quinazolinone, *Med. Chem. Res.* 18 (2009) 268–276. doi:10.1007/s00044-008-9125-0.
- [53] C. Viegas-Junior, A. Danuello, V. da Silva Bolzani, E.J. Barreiro, C.A.M. Fraga,

- Molecular hybridization: a useful tool in the design of new drug prototypes., *Curr. Med. Chem.* 14 (2007) 1829–52. <http://www.ncbi.nlm.nih.gov/pubmed/17627520> (accessed October 31, 2017).
- [54] C. Lazar, A. Kluczyk, T. Kiyota, Y. Konishi, Drug evolution concept in drug design: 1. Hybridization method., *J. Med. Chem.* 47 (2004) 6973–82. doi:10.1021/jm049637+.
- [55] M. Decker, *Design of Hybrid Molecules for Drug Development*, in: 1st editio, ELSEVIER, 2017: pp. 317–338. doi:10.1016/B978-0-08-101011-2.00025-8.
- [56] P. Venkatesh, S.N. Pandeya, Synthesis, characterisation and anti-inflammatory activity of some 2-amino benzothiazole derivatives, *Int. J. ChemTech Res.* 1 (2009) 1354–1358.
- [57] S.N. Sawhney, D.W. Boykin, Transmission of Substituent Effects in Heterocyclic Systems by Carbon- 13 Nuclear Magnetic Resonance . Benzothiazoles, *J. Org. Chem.* 44 (1979) 1136–1142.
- [58] A.J. Lin, S. Kasina, Synthesis of 3-substituted 7-(3,3-dimethyl-1-triazeno)-10-methylphenothiazines as potential antitumor agents, *J. Heterocycl. Chem.* 18 (1981) 759–761. doi:10.1002/jhet.5570180425.
- [59] Ü. Demir Özkay, Ö.D. Can, B.N. Sağlık, U. Acar Çevik, S. Levent, Y. Özkay, S. Iğın, Ö. Atlı, Design, synthesis, and AChE inhibitory activity of new benzothiazole–piperazines, *Bioorganic Med. Chem. Lett.* 26 (2016) 5387–5394. doi:10.1016/j.bmcl.2016.10.041.
- [60] Y.N. Jeong, M.Y. Choi, H.C. Choi, Preparation of Pt- and Pd-decorated CNTs by DCC-activated amidation and investigation of their electrocatalytic activities, *Electrochim.*

- Acta. 60 (2012) 78–84. doi:10.1016/j.electacta.2011.11.035.
- [61] C.-R. Lu, B. Zhao, Y.-P. Jiang, H. Ding, S. Yang, One-Pot Synthesis of Salicylanilides by Direct Amide Bond Formation from Salicyclic Acid Under Microwave Irradiation, *Synth. Commun.* 41 (2011) 1257–1266. doi:10.1080/00397911.2010.481745.
- [62] M. Colombo, S. Bossolo, A. Aramini, Phosphorus trichloride-mediated and microwave-assisted synthesis of a small collection of amides bearing strong electron-withdrawing group substituted anilines, *J. Comb. Chem.* 11 (2009) 335–337. doi:10.1021/cc900011z.
- [63] A. Leggio, E.L. Belsito, G. De Luca, M.L. Di Gioia, V. Leotta, E. Romio, C. Siciliano, A. Liguori, One-pot synthesis of amides from carboxylic acids activated using thionyl chloride, *RSC Adv.* 6 (2016) 34468–34475. doi:10.1039/C5RA24527C.
- [64] C.A.G.N. Montalbetti, V. Falque, Amide bond formation and peptide coupling, *Tetrahedron.* 61 (2005) 10827–10852. doi:10.1016/j.tet.2005.08.031.
- [65] H. Wang, H. Robinson, H. Ke, The Molecular Basis for Different Recognition of Substrates by Phosphodiesterase Families 4 and 10, *J. Mol. Biol.* 371 (2007) 302–307. doi:10.1016/j.jmb.2007.05.060.
- [66] Center for Drug Evaluation and Research: Clinical Pharmacology and Biopharmaceutics Review (S), 2009. [https://www.accessdata.fda.gov/drugsatfda\\_docs/nda/2011/022522Orig1s000ClinPharmR.pdf](https://www.accessdata.fda.gov/drugsatfda_docs/nda/2011/022522Orig1s000ClinPharmR.pdf).
- [67] D.K. Dalvie, A.S. Kalgutkar, S.C. Khojasteh-Bakht, R.S. Obach, J.P. O'Donnell,

- Biotransformation Reactions of Five-Membered Aromatic Heterocyclic Rings, *Chem. Res. Toxicol.* 15 (2002) 269–299. doi:10.1152/ajpcell.00167.2002.
- [68] A.A. Damre, K.R. Iyer, A.A. Damre, K.R. Iyer, The Significance and Determination of Plasma Protein Binding, in: *Encycl. Drug Metab. Interact.*, John Wiley & Sons, Inc., Hoboken, NJ, USA, 2012. doi:10.1002/9780470921920.edm032.
- [69] A. Daina, O. Michielin, V. Zoete, SwissADME: a free web tool to evaluate pharmacokinetics, drug-likeness and medicinal chemistry friendliness of small molecules, *Sci. Rep.* 7 (2017) 1–13. doi:10.1038/srep42717.
- [70] R.C. Garner, E.C. Miller, J.A. Miller, Liver microsomal metabolism of aflatoxin B 1 to a reactive derivative toxic to *Salmonella typhimurium* TA 1530., *Cancer Res.* 32 (1972) 2058–66. <http://www.ncbi.nlm.nih.gov/pubmed/4404160> (accessed October 20, 2017).
- [71] R. El-Bagary, H. Hashem, M. Fouad, S. Tarek, UPLC-MS-MS Method for the Determination of Vilazodone in Human Plasma: Application to a Pharmacokinetic Study, *J. Chromatogr. Sci.* 54 (2016) 1365–1372. doi:10.1093/chromsci/bmw084.

### Highlights

- New roflumilast analogues with PDE-4B inhibition activity were synthesized.
- The unsubstituted benzothiazol-2-yl and -6-yl derivatives showed a good potency.
- **6c** revealed preferential PDE-4B/4D selectivity and good % inhibition of TNF- $\alpha$ .
- **6c** showed good metabolic stability, moderate % plasma protein binding.
- **6c** binds to PDE-4B active site with additional hydrogen bonding.